

See discussions, stats, and author profiles for this publication at: <https://www.researchgate.net/publication/263944862>

Correction to “Different Plasmon Sensing Behavior of Silver and Gold Nanorods”

ARTICLE *in* JOURNAL OF PHYSICAL CHEMISTRY LETTERS · NOVEMBER 2013

Impact Factor: 7.46 · DOI: 10.1021/jz4024964

READS

40

2 AUTHORS:



Mahmoud A. Mahmoud
Georgia Institute of Technology
76 PUBLICATIONS 1,808 CITATIONS

[SEE PROFILE](#)



Mostafa A El-Sayed
Georgia Institute of Technology
676 PUBLICATIONS 55,404 CITATIONS

[SEE PROFILE](#)

Different Plasmon Sensing Behavior of Silver and Gold Nanorods

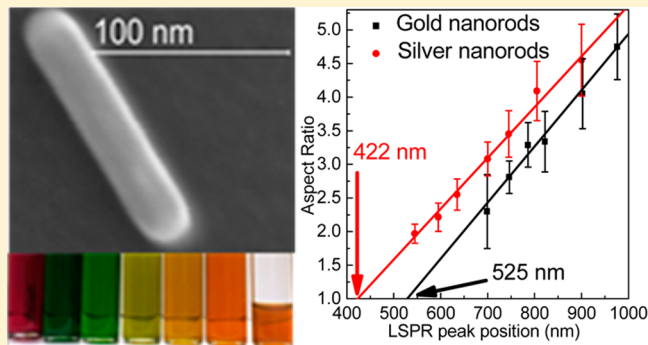
Mahmoud A. Mahmoud and Mostafa A. El-Sayed*

Laser Dynamics Laboratory, School of Chemistry and Biochemistry, Georgia Institute of Technology, Atlanta, Georgia 30332-0400, United States

Supporting Information

ABSTRACT: Silver nanorods (AgNRs) of ~20 nm diameter and different lengths, which were increased up to ~100 nm by increasing the reduction time, were prepared by a seedless synthetic approach. A linear relationship between the AgNRs aspect ratios and the LSPR peak position was observed experimentally and confirmed theoretically. The Raman signal enhancement by silver nanorods is more efficient than by gold nanorods (AuNRs) because the plasmon field intensity of AgNRs is stronger than that of AuNRs, as shown by the discrete dipole approximation calculation. The Rayleigh scattering by AuNRs is stronger than that by the AgNRs. Therefore, AuNRs are recommended for optical plasmon imaging, while AgNRs are more efficient in plasmon sensing.

SECTION: Physical Processes in Nanomaterials and Nanostructures



The optical properties of the plasmonic nanoparticles can be tuned by changing their shape,^{1,2} size,³ composition, and structure (solid or hollow).⁴ Common applications of the plasmonic metallic nanoparticles are based on the presence of the localized surface plasmon resonance (LSPR),⁵ the electromagnetic plasmon field,⁶ and the electron scavenging capability.^{7,8} Plasmonic nanoparticles have been widely used as sensors because their LSPR frequency is greatly affected by the change of the dielectric function of the surrounding medium.^{5,9} The LSPR extinction spectrum consists of two accumulated parts: absorption and scattering spectra.^{5,10} The ratio between the scattering spectrum and absorption spectrum depends on the shape, size, and composition of the plasmonic nanoparticle;¹¹ this ratio increases by increasing the particle size. The absorption part of LSPR extinction spectrum was used for the photothermal applications (biological¹² and chemical systems¹³) or in the plasmonic energy transfer to other electronic systems, which bound to the nanoparticles surface,¹⁴ while the LSPR scattering has been used to enhance the optical properties of different chemical, photochemical, and photoelectrochemical systems by light focusing.^{15,16} The electromagnetic field of the plasmonic nanoparticles is useful in enhancing different electromagnetic signals such as Raman,¹⁷ fluorescence,¹⁶ and Rayleigh scattering.¹⁸ Because of their broad applications, plasmonic nanoparticles with different shapes have been prepared by various methods, such as spheres,³ cubes,⁴ octahedrons, prisms,¹⁹ rods,² wires,^{20,21} stars,^{22,23} cages,⁴ and so on. The new designation of the plasmonic nanoparticles aims to control the following: (1) the LSPR extinction peak position to fit the application requirement, (2) the ratio between LSPR absorption and scattering spectra (some applications require strong absorption spectrum,

while strong scattering is needed in certain applications), and (3) obtaining the highest possible electromagnetic plasmon field.

Colloidal chemical techniques are efficient in the synthesis of plasmonic nanoparticles.^{24,25} Most of the plasmonic nanoparticles have been prepared by the seedless technique (formation of small nanoparticle seeds *in situ* during the nanoparticles synthesis, which grow into the characteristic shape); this technique was used to prepare different symmetrical shape nanoparticles.²⁶ The second technique is the seed-mediated method introduced by Zsigmondy,²⁷ which was based on the synthesis of the nanoparticles seeds in a separate solution and allowing them to grow in a different medium. Jana and Murphy² used this technique to prepare gold nanorods. Silver nanorods have been prepared by this seed-mediated method.^{21,28}

Plasmonic nanoparticles with NIR LSPR spectrum (such as gold nanorods²⁹ and nanocages³⁰) were used in the biological imaging because their plasmon peak does not significantly overlap with the absorption of water and biomolecules.¹² Most of the prepared plasmonic nanoparticles have plasmon resonances in the visible region, so it is useful to prepare nanoparticles with LSPR peaks in the near-infrared (NIR) regions.

Unlike many shapes of plasmonic nanoparticles, the LSPR peak position of gold nanorods²⁹ and nanocages³⁰ is independent from the particles sizes, but it depends on the ratio between the length and diameter in rods and the ratio

Received: March 6, 2013

Accepted: April 18, 2013

Published: April 18, 2013

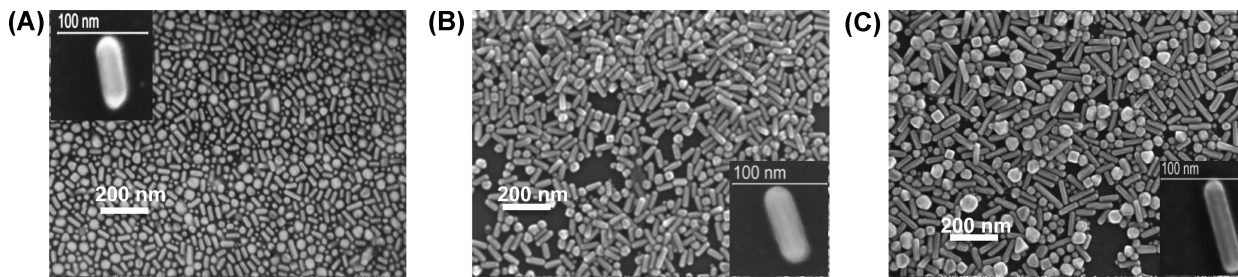


Figure 1. SEM images of silver nanorods of different length (A) 44.9 ± 4.7 , (B) 64.1 ± 5.6 , and (C) 86.0 ± 9.7 . The insets show the magnified images of single nanorods.

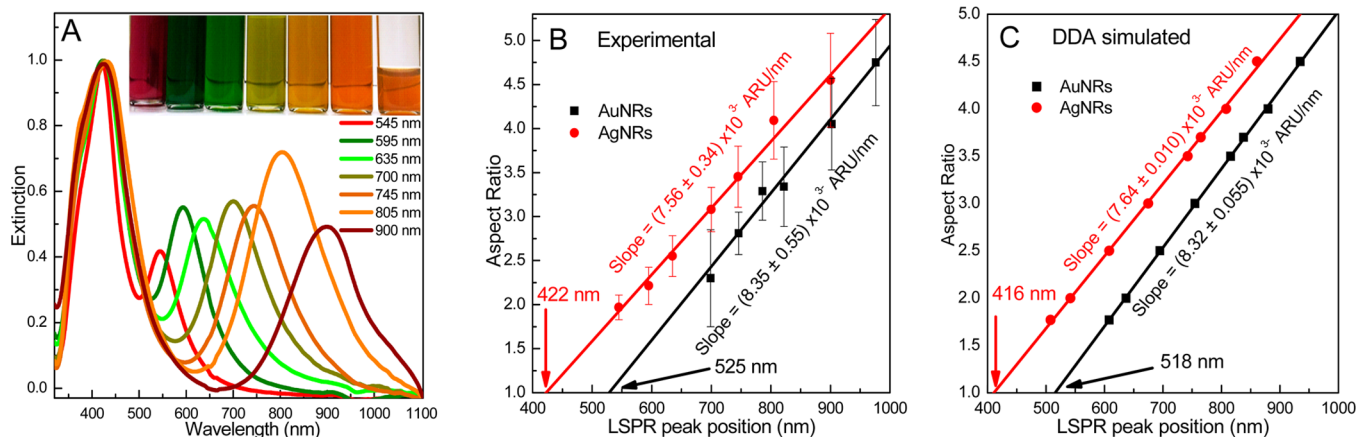


Figure 2. (A) LSPR spectra of AgNRs of different aspect ratios dispersed in water medium; the inset picture is for the AgNRs. Red shift in the LSPR peak is observed as the length of the rods is increased. (B) Relationship between the aspect ratios of AgNRs and AuNRs with diameter of ~ 21 nm and the LSPR peak positions. When the aspect ratio is unity (sphere) the peak positions are at 422 and 525 nm for AgNRs and AuNRs, respectively. (C) Relationship between the aspect ratios of AgNRs and AuNRs with 21 nm diameter and the LSPR peak positions calculated by the DDA simulation.

between the length and thickness in nanocages.⁹ Although the LSPR peak of gold nanorods and nanocages is in the NIR region, gold rods are characterized by the presence of two LSPR peaks, while the cages have only one plasmon peak. Moreover, opposite to the AgNRs, the LSPR peak of gold cages can be tuned without changing the outer volume but by changing the wall thickness. Most of the optical applications of plasmonic nanoparticles, such as Raman signal enhancement, rely on the nanoparticles' plasmon fields (according to the electromagnetic mechanism).⁶ This letter presents a new synthetic technique for the preparation of colloidal silver nanorods of similar diameter but with different aspect ratios (ARs) based on the seedless technique. The optical properties of gold and silver nanorods are compared experimentally and theoretically by the discrete dipole approximation (DDA) simulation. The Raman enhancement by silver and gold nanorods of comparable ARs is also discussed theoretically and experimentally as well.

Silver nanorods of different ARs were prepared by ethylene glycol (EG, purchased from BDH) reduction of silver salt ($\text{AgNO}_3 \geq 99\%$, Sigma) in the presence of polyvinylpyrrolidone (PVP) (MW 55 000g, Sigma) capping agent at high temperature and stirring speed. In brief, 70 mL of EG was heated to 140 °C for 1 h on a round-bottomed glass flask. After heating for 1 h, the temperature was increased to 175 °C and 0.5 g PVP was added to the EG solution. The resulting solution was stirred at 1600 rpm and a solution of AgNO_3 (0.15 g dissolved in 3 mL of EG) was injected, then the stirring was continued for 5 min. Then, the flask was covered well by a glass

cover until the color of the solution turned slightly pink. The color of the solution was changed, under stirring speed of 1600 rpm, with time due to the elongation of the silver nanorods. Therefore, every 15 s, 10 mL from the reaction mixture was transferred to a 20 mL glass vial cooled with ice-water solution. The color of samples changed with time in the following order: red, green, olive, brownish, tan, and opaque yellow. The silver nanorods were cleaned by dilution with deionized water (DI) and centrifuging at 13 000 rpm for 20 min, followed by dispersion of the precipitate in DI water. The sample was re-centrifuged at 10 000 rpm for 10 min and finally dispersed in DI water. Gold nanorods (AuNRs) were prepared as described by the Murphy and El-Sayed groups.^{2,24} An Ocean Optics HR4000Cg-UV-NIR was used to measure the optical properties of the cleaned AgNRs dispersed in water. A Zeiss Ultra 60 was used for the scanning electron microscopy (SEM) imaging. The Raman experiment was conducted using a Renishaw Invia Raman microscope with 4-nitrothiophenol (4NTP) adsorbed on the surface of AgNRs and AuNRs. Two mL of aqueous solution of 4NTP (0.5 μM) was mixed with 2 mL of AgNRs or AuNRs (OD = 2). After 3 h, the resulting solutions were centrifuged at 6000 rpm for 10 min and the precipitate was dispersed in 1 mL of DI water and then centrifuged at 6000 for 5 min. The precipitate was dispersed in 0.5 mL of DI water and transferred to a 2 mm thick quartz cell for Raman measurement (to avoid dryness of the sample).

Characterization of Silver Nanorods. As-prepared silver nanorods solutions appeared in different colors depend on their ARs. Unlike symmetrical shape plasmonic nanoparticles,

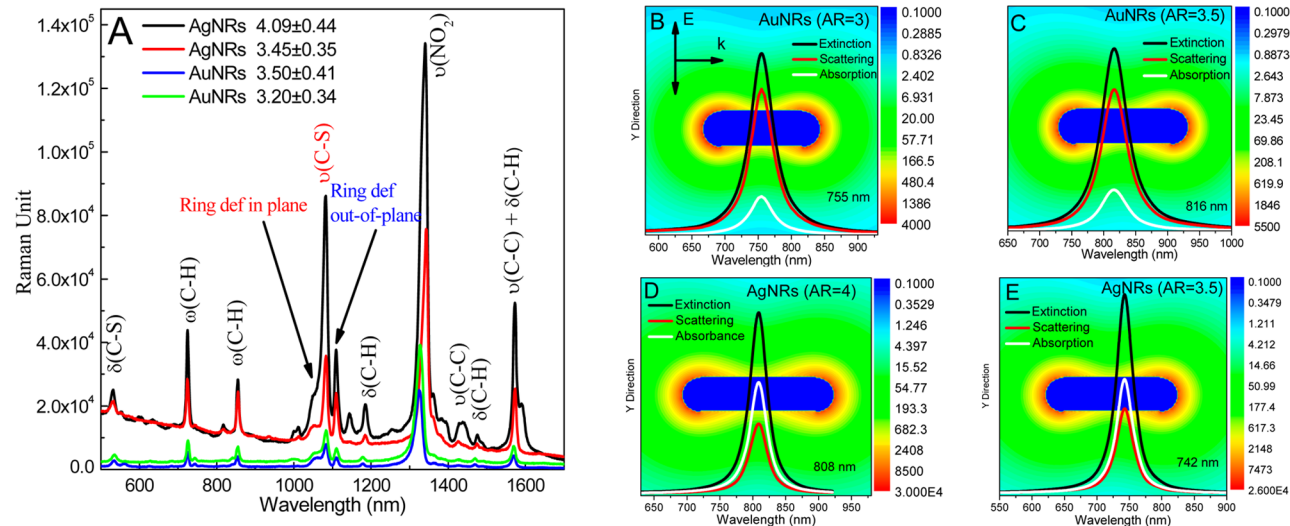


Figure 3. (A) SERS of 4-nitrothiophenol adsorbed on the surface of AuNRs and AgNRs with different aspect ratios. Plasmon field contour, simulated by DDA calculation, of AuNRs and AgNRs of diameter of 22 nm and different aspect ratio: (B) AuNRs of 3 aspect ratio, (C) AgNRs of 3.5 aspect ratio, and (D) AgNRs of 4 aspect ratio. The spectra in panels B–E are extinction spectrum (black), scattering spectrum (red), and absorption (white).

in which their LSPR peak position red shifts as their size increases, the LSPR peak position of rod-shaped noble metal plasmonic nanoparticles depends on their AR (the ratio between the length and width of the nanorods). Therefore, one cannot estimate the nanoparticle size of the nanorods shape as in symmetrical nanoparticle shapes. Before using the plasmonic nanoparticles of rod shape in any application, electronic imaging and statistical analysis have to be carried out. The SEM images of AgNRs prepared at different reduction times are shown in Figure 1A–C and Figure S1 in the Supporting Information. The inset of each SEM image shows the magnified image of a single rod. Statistical analysis for the lengths and diameters of 300 AgNRs, which are taken from multiple SEM images of each samples, shows that the diameters (D) of the AgNRs do not change much with increasing the reduction time but the length (L) increases. The specifications of the prepared AgNRs are changed as the reduction time increases in the following order: $L = 39.6 \pm 3.2$ nm and $D = 20.1 \pm 1.7$ nm, $L = 44.9 \pm 4.7$ nm and $D = 20.3 \pm 1.1$ nm (Figure 1A), $L = 55.5 \pm 5.5$ nm and $D = 21.7 \pm 1.7$ nm, $L = 64.1 \pm 5.6$ nm and $D = 20.8 \pm 1.6$ nm (Figure 1B), $L = 73.5 \pm 7.8$ nm and $D = 21.3 \pm 1.7$ nm, $L = 86.0 \pm 9.7$ nm and $D = 21.1 \pm 1.7$ nm (Figure 1C), and $L = 101.1 \pm 12.4$ nm and $D = 22.2 \pm 1.9$ nm, respectively. Therefore, the AR of the prepared AgNRs increases as the reduction time increased in the following trend: 1.97 ± 0.14 , 2.21 ± 0.21 , 2.55 ± 0.23 , 3.08 ± 0.25 , 3.45 ± 0.35 , 4.09 ± 0.44 , and 4.55 ± 0.53 , respectively.

Optical Properties of Silver Nanorods with Different Aspect Ratios. The optical and sensing applications of the plasmonic nanoparticles are based on their LSPR extinction peaks and plasmon fields. Plasmonic nanoparticles with rod shape are characterized by the presence of two LSPR plasmon peaks^{2,24} corresponding to the longitudinal and transverse electron oscillation modes. Figure 2A shows the LSPR spectrum of AgNRs taken from the solution during the synthesis at different reduction times. The LSPR spectrum of AgNRs transverse LSPR peak is in the range of 400 nm, while the longitudinal LSPR peak shifts to longer wavelengths as the AR increases. The LSPR peak at 400 nm corresponds to both the transverse

mode of AgNRs and the LSPR of the nanorod shapes such as spheres and cubes. The relationships between the AR and the longitudinal LSPR peak position of AgNRs and AuNRs with the same diameter are shown in Figure 2B. The values of the ARs and the LSPR peak position of the AuNRs are obtained from a previous study.³¹ This relationship between the AR and the LSPR for AgNRs and AuNRs is fitted linearly. When the AR = 1 (spherical shape), the LSPR peak position will be at 422 and 525 nm for AgNRs and AuNRs, respectively. To confirm the experimental relationship between the AR and the LSPR peak positions, we carried out the DDA simulation to calculate the LSPR extinction peak positions of both AgNRs and AuNRs of different AR. Similar to the experimental results, this relationship (AR versus LSPR peak position) is linear with slopes matching the experimental values. (See Figure 2C.)

SERS sensing by AgNRs vs AuNRs. The plasmon field of the plasmonic nanoparticles enhances the Raman signal of molecules present in its domain (electromagnetic mechanism).⁶ The efficiency of Raman enhancement by the plasmonic nanoparticles increases as the plasmon field increases. Therefore, the degree of Raman enhancement by the plasmonic nanoparticles gives an indication of their plasmon field intensity. To determine the Raman enhancement ability of AgNRs compared with AuNRs the Raman band intensities of 4NTP adsorbed on the particles' surfaces were measured. AgNRs and AuNRs were used with two different ARs for each.³² Figure 3A shows the SERS spectrum of 4NTP adsorbed on the surface of AgNRs with AR of 3.45 ± 0.35 and 4.09 ± 0.44 and on AuNRs of 3.20 ± 0.34 and 3.50 ± 0.41 AR. The SEM images of AuNRs of the two AR are shown in Figure S2 in the Supporting Information. The LSPR spectrum of both AgNRs and AuNRs are broad enough to be excited by a 785 nm Raman laser. The LSPR peak positions of AgNRs of 3.45 ± 0.35 and 4.09 ± 0.44 AR are centered at 745 and 805 nm, respectively, after coating with 4NTP, while the LSPR peak positions for AuNRs of 3.20 ± 0.34 and 3.50 ± 0.41 AR are at 755 and 805 nm, respectively, after coating with 4NTP (Figure S3 in the Supporting Information). It is observed that the SERS enhancement by AgNRs is stronger than that by AuNRs for

both ARs; the SERS enhancement factor for AgNRs is (~ 0.1 to 2.0×10^{14} , while for AuNRs it is (~ 0.3 to 2.2×10^{12} . Moreover, the longer rods showed ~ 10 times better enhancement than the shorter ones for both of the two metals. A silver nanosphere has been reported to be a better Raman enhancer than gold nanospheres as the interband transition of gold nanoparticles overlaps with their LSPR peaks, causing plasmon energy loss, but for AuNRs and AgNRs, the longitudinal LSPR is far from the interband transition in both gold and silver, so this cannot be the reason for the observed difference. Moreover, the LSPR of silver is sharper than that of gold, which indicates that the oscillation coherence time in silver is longer than that in gold and that the plasmon field of silver is accordingly stronger.³³

The efficiency of the plasmonic nanoparticles as sensor can be determined by the sensitivity factor (the amount of shift in the LSPR peak position per unit change in the refractive index of the surrounding medium). The amount of shift in the LSPR peak of AgNRs and AuNRs after coating with 4NTP can be used to compare the sensing efficiency of AgNRs and AuNRs. The LSPR peak of AuNRs and AgNRs was red-shifted after coating with 4NTP. This red shift was found to be 10 and 14 nm for AgNRs of AR of 3.45 ± 0.35 and 4.09 ± 0.44 , respectively, while for AuNRs of AR of 3.20 ± 0.34 and 3.50 ± 0.41 the red shift was 1 and 8 nm, respectively. In general, the red shift in the case of AgNRs is higher than that in the case of AuNRs. This means the sensitivity factor value of AgNRs is higher than that of AuNRs of comparable size. This result confirms that the Raman measurements proved that AgNRs are better sensors than AuNRs.

DDA calculation was carried out to calculate the LSPR extinction, absorption, and scattering as well as the electromagnetic plasmon field for both AgNRs and AuNRs (spectra in Figure 3B–E and Figure 4S in the Supporting Information). The LSPR spectrum of AgNRs is narrower than that of AuNRs. Moreover, the LSPR of AuNRs is dominated by scattering, while the absorption dominates in the AgNRs spectrum. This calculation agrees well with the fact that AuNRs appear much brighter than AgNRs when they interact with the laser during the Raman measurement due to higher scattering. Figure 4

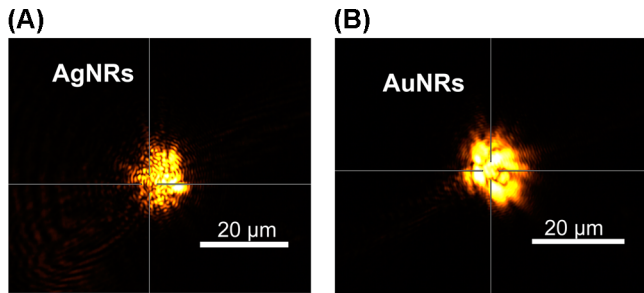


Figure 4. Rayleigh scattering of the 785 nm laser by (A) AgNRs and (B) AuNRs. The Rayleigh scattering intensity by AuNRs is stronger than that by AgNRs.

shows the Rayleigh scattering for the 785 nm laser by AgNRs (AR = 4.09 ± 0.44) and AuNRs (AR = 3.5 ± 0.41). The scattering intensity by AuNRs seems to be much stronger than that of AgNRs.

DDA was also used to calculate the plasmon field intensity and distribution. This showed why AgNRs produce a stronger SERS enhancement than AuNRs. Figure 3B–D shows the

plasmon field contour of AgNRs of 3.5 and 4 AR and AuNRs of 3.5 and 4 AR. When the longitudinal mode is excited, the plasmon field calculated by DDA simulation of AgNRs is found to be five times higher than that of AuNRs of the same AR. The plasmon field intensity increases as the AR increases.

In summary, silver nanorods have been prepared by a new seedless colloidal chemical approach. The longitudinal plasmon peak position of silver nanorods prepared by this method can be tuned from 500 to 1000 nm. The relationship between the AR and the plasmon peak position of silver nanorods is linear, and this is useful in predicting the AR for any silver nanorods of known surface plasmon peak position and vice versa. The silver nanorods showed Raman enhancement greater than gold nanorods of comparable ARs and diameters. The theoretical calculations of the plasmon field intensity are in good agreement with the Raman measurement and support the idea that the electromagnetic plasmon field intensity of silver nanorods is stronger than that of the gold nanorods. The intensity of the scattering peak in gold nanorods is higher than that of the silver nanorods. The estimated sensitivity factor of silver nanorods is higher than that of gold nanorods.

■ ASSOCIATED CONTENT

S Supporting Information

Figure S1 is SEM image of AgNR with four different ARs. Figure S2 is SEM image of AuNRs of two different aspect ratios. Figure S3 is LSPR spectrum of AgNRs and AuNRs before and after coating with *p*-nitrothiophenol. Figure S4 is the LSPR extinction, scattering, and absorption spectra of AgNRs and AuNRs of different ARs, calculated by the DDA calculation. This material is available free of charge via the Internet at <http://pubs.acs.org>.

■ AUTHOR INFORMATION

Corresponding Author

*E-mail: melsayed@gatech.edu.

Notes

The authors declare no competing financial interest.

■ ACKNOWLEDGMENTS

The authors would like to thank the DOE for financial support from Grant No. DE-FG02-97-ER 14799.

■ REFERENCES

- (1) Jin, R. C.; Cao, Y. W.; Mirkin, C. A.; Kelly, K. L.; Schatz, G. C.; Zheng, J. G. Photoinduced Conversion of Silver Nanospheres to Nanoprisms. *Science* **2001**, *294*, 1901–1903.
- (2) Jana, N. R.; Gearheart, L.; Murphy, C. J. Wet Chemical Synthesis of High Aspect Ratio Cylindrical Gold Nanorods. *J. Phys. Chem. B* **2001**, *105*, 4065–4067.
- (3) Freund, P. L.; Spiro, M. Colloidal Catalysis - the Effect of Sol Size and Concentration. *J. Phys. Chem.* **1985**, *89*, 1074–1077.
- (4) Sun, Y. G.; Xia, Y. N. Shape-Controlled Synthesis of Gold and Silver Nanoparticles. *Science* **2002**, *298*, 2176–2179.
- (5) Kelly, K. L.; Coronado, E.; Zhao, L. L.; Schatz, G. C. The Optical Properties of Metal Nanoparticles: The Influence of Size, Shape, and Dielectric Environment. *J. Phys. Chem. B* **2003**, *107*, 668–677.
- (6) Jeanmaire, D. L.; Vanduyne, R. P. Surface Raman Spectroelectrochemistry 0.1. Heterocyclic, Aromatic, and Aliphatic-Amines Adsorbed on Anodized Silver Electrode. *J. Electroanal. Chem.* **1977**, *84*, 1–20.
- (7) Dawson, A.; Kamat, P. V. Semiconductor-Metal Nanocomposites. Photoinduced Fusion and Photocatalysis of Gold-Capped TiO₂ (TiO₂/Gold) Nanoparticles. *J. Phys. Chem. B* **2001**, *105*, 960–966.

- (8) Mahmoud, M. A.; Qian, W.; El-Sayed, M. A. Following Charge Separation on the Nanoscale in Cu₂O-Au Nanoframe Hollow Nanoparticles. *Nano Lett.* **2011**, *11*, 3285–3289.
- (9) Mahmoud, M. A.; El-Sayed, M. A. Gold Nanoframes: Very High Surface Plasmon Fields and Excellent Near-Infrared Sensors. *J. Am. Chem. Soc.* **2010**, *132*, 12704–12710.
- (10) Mahmoud, M. A.; Chamanzar, M.; Adibi, A.; El-Sayed, M. A. Effect of the Dielectric Constant of the Surrounding Medium and the Substrate on the Surface Plasmon Resonance Spectrum and Sensitivity Factors of Highly Symmetric Systems: Silver Nanocubes. *J. Am. Chem. Soc.* **2012**, *134*, 6434–6442.
- (11) Lee, K. S.; El-Sayed, M. A. Gold and Silver Nanoparticles in Sensing and Imaging: Sensitivity of Plasmon Response to Size, Shape, and Metal Composition. *J. Phys. Chem. B* **2006**, *110*, 19220–19225.
- (12) Huang, X. H.; El-Sayed, I. H.; Qian, W.; El-Sayed, M. A. Cancer Cell Imaging and Photothermal Therapy in the Near-Infrared Region by Using Gold Nanorods. *J. Am. Chem. Soc.* **2006**, *128*, 2115–2120.
- (13) Govorov, A. O.; Zhang, W.; Skeini, T.; Richardson, H.; Lee, J.; Kotov, N. A. Gold Nanoparticle Ensembles as Heaters and Actuators: Melting and Collective Plasmon Resonances. *Nanoscale Res. Lett.* **2006**, *1*, 84–90.
- (14) Liu, G. L.; Long, Y. T.; Choi, Y.; Kang, T.; Lee, L. P. Quantized Plasmon Quenching Dips Nanospectroscopy via Plasmon Resonance Energy Transfer. *Nat. Methods* **2007**, *4*, 1015–1017.
- (15) Mahmoud, M. A.; El-Sayed, M. A. Plasmonic Field Effects on the Energy Transfer between Poly(p-phenyleneethynylene) Fluorescent Polymer and Au Nanocages. *J. Phys. Chem. C* **2011**, *115*, 12726–12735.
- (16) Mahmoud, M. A.; Poncheri, A. J.; Phillips, R. L.; El-Sayed, M. A. Plasmonic Field Enhancement of the Exciton-Exciton Annihilation Process in a Poly(p-phenyleneethynylene) Fluorescent Polymer by Ag Nanocubes. *J. Am. Chem. Soc.* **2010**, *132*, 2633–2641.
- (17) Zhao, J.; Dieringer, J. A.; Zhang, X. Y.; Schatz, G. C.; Van Duyne, R. P. Wavelength-Scanned Surface-Enhanced Resonance Raman Excitation Spectroscopy. *J. Phys. Chem. C* **2008**, *112*, 19302–19310.
- (18) Blaber, M. G.; Henry, A. I.; Bingham, J. M.; Schatz, G. C.; Van Duyne, R. P. LSPR Imaging of Silver Triangular Nanoprisms: Correlating Scattering with Structure Using Electrodynamics for Plasmon Lifetime Analysis. *J. Phys. Chem. C* **2012**, *116*, 393–403.
- (19) Millstone, J. E.; Hurst, S. J.; Metraux, G. S.; Cutler, J. I.; Mirkin, C. A. Colloidal Gold and Silver Triangular Nanoprisms. *Small* **2009**, *5*, 646–664.
- (20) Tao, A.; Kim, F.; Hess, C.; Goldberger, J.; He, R. R.; Sun, Y. G.; Xia, Y. N.; Yang, P. D. Langmuir-Blodgett Silver Nanowire Monolayers for Molecular Sensing using Surface-Enhanced Raman Spectroscopy. *Nano Lett.* **2003**, *3*, 1229–1233.
- (21) Zhang, J.; Langille, M. R.; Mirkin, C. A. Synthesis of Silver Nanorods by Low Energy Excitation of Spherical Plasmonic Seeds. *Nano Lett.* **2011**, *11*, 2495–2498.
- (22) Nehl, C. L.; Liao, H. W.; Hafner, J. H. Optical Properties of Star-Shaped Gold Nanoparticles. *Nano Lett.* **2006**, *6*, 683–688.
- (23) Mahmoud, M. A.; Tabor, C. E.; El-Sayed, M. A.; Ding, Y.; Wang, Z. L. A New Catalytically Active Colloidal Platinum Nanocatalyst: The Multiarmed Nanostar Single Crystal. *J. Am. Chem. Soc.* **2008**, *130*, 4590–4591.
- (24) Nikoobakht, B.; El-Sayed, M. A. Preparation and Growth Mechanism of Gold Nanorods (NRs) Using Seed-Mediated Growth Method. *Chem. Mater.* **2003**, *15*, 1957–1962.
- (25) Grzelczak, M.; Perez-Juste, J.; Mulvaney, P.; Liz-Marzan, L. M. Shape Control in Gold Nanoparticle Synthesis. *Chem. Soc. Rev.* **2008**, *37*, 1783–1791.
- (26) Turkevich, J.; Stevenson, P. C.; Hillier, J. A Study of The Nucleation and Growth Processes in the Synthesis of Colloidal Gold. *Discuss. Faraday Soc.* **1951**, *55*–75.
- (27) Zsigmondy, R. *The Chemistry of Colloids*; John Wiley & Sons, Inc.: New York, 1917.
- (28) Pietrobon, B.; McEachran, M.; Kitaev, V. Synthesis of Size-Controlled Faceted Pentagonal Silver Nanorods with Tunable Plasmonic Properties and Self-Assembly of These Nanorods. *ACS Nano* **2009**, *3*, 21–26.
- (29) El-Sayed, I. H.; Huang, X. H.; El-Sayed, M. A. Selective Laser Photo-Thermal Therapy of Epithelial Carcinoma Using Anti-EGFR Antibody Conjugated Gold Nanoparticles. *Cancer Lett.* **2006**, *239*, 129–135.
- (30) Skrabalak, S. E.; Au, L.; Lu, X. M.; Li, X. D.; Xia, Y. N. Gold Nanocages for Cancer Detection and Treatment. *Nanomedicine* **2007**, *2*, 657–668.
- (31) Hu, M.; Wang, X.; Hartland, G. V.; Mulvaney, P.; Juste, J. P.; Sader, J. E. Vibrational Response of Nanorods to Ultrafast Laser Induced Heating: Theoretical and Experimental Analysis. *J. Am. Chem. Soc.* **2003**, *125*, 14925–14933.
- (32) Orendorff, C. J.; Gearheart, L.; Jana, N. R.; Murphy, C. J. Aspect Ratio Dependence on Surface Enhanced Raman Scattering Using Silver and Gold Nanorod Substrates. *Phys. Chem. Chem. Phys.* **2006**, *8*, 165–170.
- (33) Wokaun, A.; Gordon, J. P.; Liao, P. F. Radiation Damping in Surface-Enhanced Raman-Scattering. *Phys. Rev. Lett.* **1982**, *48*, 957–960.